

PHENOMENOLOGY OF SURFACE ARCS ON SPACECRAFT DIELECTRIC MATERIALS

K G Balmain, M Gossland & R D Reeves

*Department of Electrical Engineering
University of Toronto, Canada*

W G Kuller

*US Air Force
Weapons Laboratory, Albuquerque, USA*

ABSTRACT

For electron beam incidence on large specimens of Kapton thermal blanket material, surface arc discharges are shown to cause damage consisting of punchthrough holes which act as focal points for other types of damage, including subsurface tunnels, blowout holes and surface breakup. Under electron bombardment, dielectric sheet specimens separated by a gap are shown to discharge simultaneously. Teflon specimens which have been brushed or rubbed are shown to exhibit directional guidance of discharge arcs, and this phenomenon has been used to generate straight arcs whose velocities have been measured optically.

Keywords: Dielectric Arc Propagation, Dielectric Arc Damage, Dielectric Flashover, Spacecraft Discharge, Spacecraft Charging.

1. ARC DAMAGE ON KAPTON

Kapton is widely used as the outer layer of spacecraft thermal blankets. It is known that, when monoenergetic 25 keV nonpenetrating electron beams are incident on large areas of 50 μm thick Kapton, very strong surface arc discharges can occur (Ref. 1), each discharge draining a large fraction of the accumulated surface charge. When high energy electrons are added to the low energy ones at 20-25 keV, discharges cease in some situations (200 keV electrons at 100 pA/cm²: Ref. 2), but discharges occur and can become stronger in other situations (β -decay spectrum of Strontium-90 at 5 pA/cm²: Ref. 3).

A sample of the 90 cm diameter, 50 μm thick aluminized Kapton specimen used in Ref. 2 was searched for traces of damage caused by the arcs which occurred during periods when the high energy beam was not on and only 25 keV electrons at up to 13 nA/cm² were incident on the material. At one point located centrally on the specimen, a punchthrough arc had perforated the Kapton sheet and blown off the nearby aluminized backing. The perforation and surrounding "crater" are shown in Figures 1 and 2. Opening into the crater are holes, one of which is shown in Figure 3 with a small blowout hole nearby,

and the blowout hole is shown magnified in Figure 4. Light microscope photographs with surface focus (Figure 5) and subsurface focus (Figure 6) show that the crater opening is linked to the blowout hole by a "tunnel" perhaps 5 μm below the surface. A larger crater opening with three blowout holes connected by a tunnel are shown in Figures 7 through 12. The blowout holes and crater openings show signs of melting, but much of the nearby surface damage appears to be surface bubbles which have heaved up and burst. Therefore both molten and gaseous substances have been ejected.

While this localized damage on the specimen is considerable, its occurrence over the surface is rare. Only a tiny percentage of the total surface shows unambiguous microscopic evidence of damage, compared with unexposed material. Furthermore, around the punchthrough, only four well-defined tunnels were found. It would appear that the punchthrough, once formed, becomes the focal point for high charge accumulation and for the initiation of propagating surface discharges accompanied by tunnel formation in regions of high arc current density. In other experiments at higher current densities in which punchthrough did not occur, damage appears to be much more widespread (Ref. 4). These observations on discharge damage are consistent with both visual and current pulse observations that punchthrough occurrence is followed by weaker and more frequent discharges which converge on the punchthrough site.

2. ARC TRIGGERING ACROSS A GAP

Figure 13 shows a single discharge event on two separate sheets of Mylar. This experiment had been intended to demonstrate the directional preference of discharge arcs, the method being to cut a square specimen in two and rotate half by ninety degrees. A clear directional dependence is evident, and this subject was studied in subsequent work (Ref. 5). What was unexpected was the apparent simultaneity of arcs on the two pieces of dielectric, suggesting that the arc on one piece produced a combination of fields and particles which triggered the arc on the other piece, across a gap of about 4 millimetres.

A series of controlled experiments was carried out involving two adjacent pieces of 125 μm thick, spacecraft grade silvered Teflon tape. The pieces were covered by a mask such that the only exposed edges were the adjacent edges. Visual observation

indicated that arc initiation always occurred at an exposed edge, and that the arcs occurred sometimes on one specimen, sometimes on the other, and sometimes on both at the same time. The percentage occurrence of apparently simultaneous arcs on the two materials proved to be a function of gap width as can be seen in the following table.

Gap Width (mm)	Number of Specimens	Number of Discharges	% Occurrence of Simultaneous Arcs: by specimens; averages.	
.5	1	23	91	91
1.0	2	22,35	18.2, 77.0	47.6
1.5	2	44,33	52.3, 33.3	42.8
2.0	2	9,58	11.1, 6.9	9.0
2.5	2	38,70	0, 10.0	5.0

The average percent occurrence of simultaneous arcs decreases monotonically with increasing gap width, suggesting the existence of a well-defined coupling mechanism which diminishes with distance.

3. ARC DIRECTION CONTROL

By accident, it was discovered that attempts to clean a Teflon specimen surface by means of very light brushing with a soft brush resulted in control over arc direction, and similar observations following surface rubbing have been made in the course of experiments at NASA Lewis Research Center (N.J. Stevens and J.V. Staskus: personal communication). Figure 14 shows an arc on a 50 μ m thick Teflon specimen with no surface treatment: no strong directionality is evident. Figure 15 shows the arc pattern resulting from very light circular brushing. Subsequently the specimen of Figure 15 was brushed horizontally resulting in the arc pattern of Figure 16, and then brushed vertically resulting in the arc pattern of Figure 17. Each arc pattern is for a single discharge event.

Similar arc guidance effects on Teflon followed light rubbing with acetone-wetted lens-cleaning tissue. By this method, both straight arcs and zig-zag arcs were readily produced. Microscopic examination of these discharged specimens revealed faint sub-micron-width "scratches" apparently caused by the rubbing, but no sign at all of the branching or "leafy" grooves and tunnels which are frequently observed forms of damage on specimens with no surface treatment.

Arc guidance could be caused by either surface scratching or by the laying down of friction-generated stripes of charge. Two-dimensional computations of charge accumulation patterns (Ref.6) show that a step change in dielectric thickness produces a sharp peak in both accumulated charge and electric field at the step: such a step change in thickness could be a partial simulation of a

surface scratch. Also, computations for both positive and negative pre-charged stripes (Ref.7) show charge and field peaks along the stripe edges. In both the above computations the charge and field peaks grew and persisted throughout the charge-up period, indicating that discharge initiation would occur preferentially along the high-field lines.

4. ARC VELOCITY MEASUREMENT

The optical measurement of arc velocity requires the occurrence of straight, single arcs. It has already been shown that rubbing or brushing in a straight line produces straight discharge arcs. However, multiple arcs are the rule rather than the exception and they cannot be used for velocity measurement. Computations (Refs.6,7) show that the embedded charge density in a beam-charged dielectric strip is maximum along its centre-line, so it was reasoned that a metal mask with a long, narrow aperture laid over the specimen would produce the desired effect. This postulate proved to be correct, with mask aperture widths of about 5 mm being adequately narrow to produce single arcs fairly consistently. Two optical fibers lying under the aperture mask carried the light impulses to a pair of avalanche photodiode detectors and a 400 MHz dual-beam oscilloscope, an arrangement which permitted the arc velocity to be deduced directly. The only other experimental requirement was that the arc start near either end of the mask aperture and definitely not between the optical fibers; this was assured by creating an initiation point (such as a pinprick) near one end of the specimen.

An extensive set of measurements was carried out on 125 μ m thick silvered Teflon tape, using a 20 keV electron beam with a current density of 100 nA/cm². The measured light pulses had risetimes of the order of 20 ns and decay times of the order of 120 ns: only the rising part of the pulse was used for velocity measurement. The required time differences were established in two ways a) by noting the departure of the pulse by a fixed amount from the baseline and b) by noting the intersection of the baseline with an extrapolated straight line drawn through the fastest-rising part of the pulse trace: the mean velocities deduced from the two methods were not significantly different, so the results from both methods are included in Figure 18. Preliminary measurements of velocity for half the Teflon thickness (60 μ m) were not significantly different, and there was no evidence of fatigue effects.

The mean velocity of 7.1×10^5 m/s should be compared with other experimental estimates which involved dividing the specimen dimensions by the duration of the discharge current pulse. Such estimates for Teflon are usually in the range of 1.5×10^5 m/s to 3.0×10^5 m/s (see for example Ref.8). A theoretical prediction of 1.65×10^5 m/s (Ref.9) comes from computing the evolution of negative streamer breakdown and likening it to the early stages of a dielectric arc. The present experimental result is significantly faster, a partial explanation for which may be the straightness of the measured arc.

5. ACKNOWLEDGMENT

The photography and experimentation were done in

part by G.R. Dubois. The research was supported by the U.S. Air Force Weapons Laboratory and by NASA, under NASA Grant NSG-7647, and by the Natural Sciences and Engineering Research Council of Canada under Grant A-4140.

6. REFERENCES

1. Flanagan, T.M., Denson, R., Mallon, C.E., Treadaway, M.J., and Wenaas, E.P. 1979, Effect of laboratory simulation parameters on spacecraft dielectric discharges, IEEE Trans. Nucl. Sci. Vol. NS-26, No.6, 5134-5140.
2. Treadaway, M.J., Mallon, C.E., Flanagan, T.M., Denson, R., and Wenaas, E.P. 1979, The effects of high energy electrons on the charging of spacecraft dielectrics, IEEE Trans. Nucl. Sci. Vol. NS-26, No.6, 5102-5106.
3. Balmain, K.G., and Hirt, W. 1980, Dielectric surface discharges: effects of combined low-energy and high-energy incident electrons, Spacecraft Charging Technology 1980, NASA CP-2182/AFGL-TR-81-0270, 115-128.
4. Balmain, K.G. 1979, Surface discharge arc propagation and damage on spacecraft dielectrics, Spacecraft Materials in Space Environment, ESA SP-145, pp. 209-215.
5. Gossland, M., Balmain, K.G., and Treadaway, M. J. 1981, Surface flashover arc orientation on Mylar film, IEEE Trans. Nucl. Sci. Vol. NS-28, No.6, 4535-4540.
6. Reeves, R.D., and Balmain, K.G. 1981, Two-dimensional electron beam charging model for polymer films, IEEE Trans. Nucl. Sci. Vol. NS-28, No.6, 4547-4552.
7. Reeves, R.D. 1981, Two-dimensional electron beam charging model for polymer films, M.A.Sc. Thesis, Department of Electrical Engineering, University of Toronto.
8. Balmain, K.G., and Dubois, G.R. 1979, Surface discharges on Teflon, Mylar and Kapton, IEEE Trans. Nucl. Sci. Vol. NS-26, No.6, 5146-5151.
9. Beers, B.L., Pine, V.W., Hwang, H.C., and Bloomberg, H.W. 1979, Negative streamer development in FEP Teflon, IEEE Trans. Nucl. Sci. Vol. NS-26, No.6, 5127-5133.

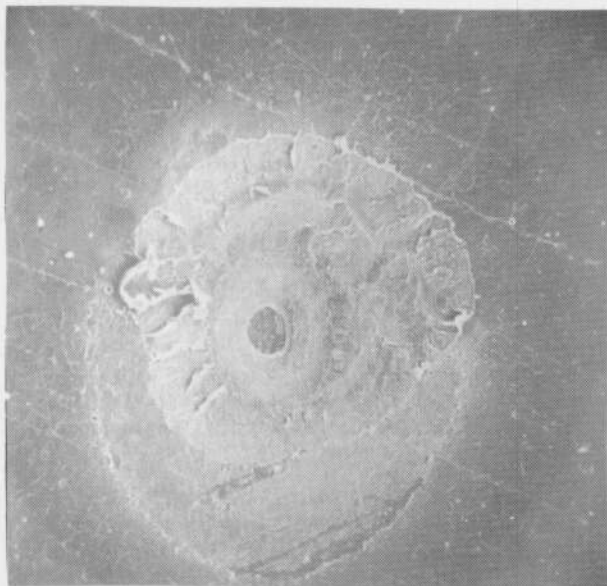


Fig.1 Kapton SEM image : 100 μm

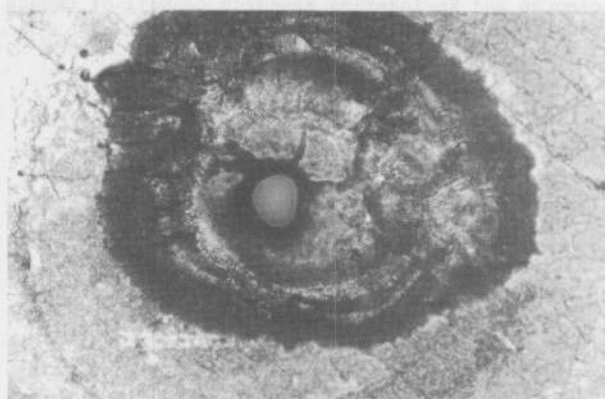


Fig.2 Reflected light : 100 μm

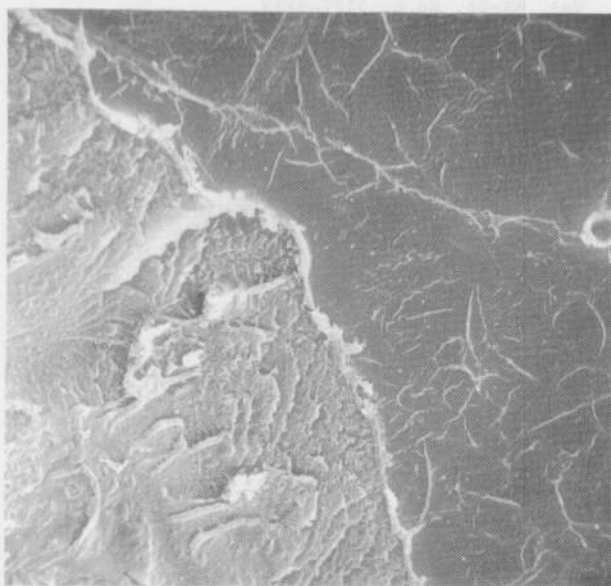


Fig.3 SEM image : 10 μm

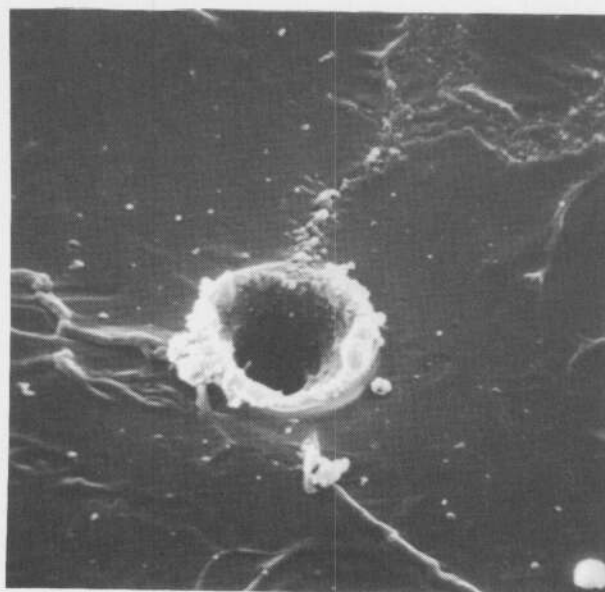


Fig.4 SEM image : 5 μm

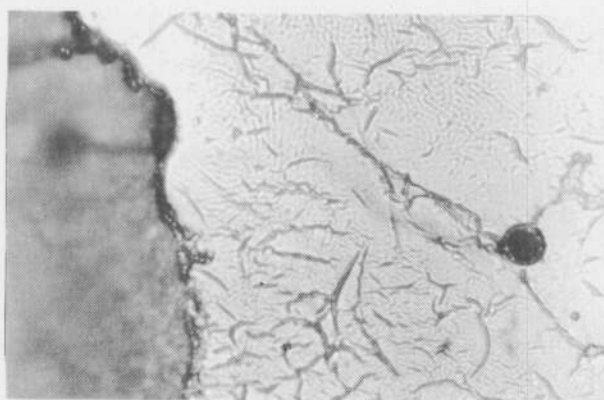


Fig.5 Reflected light : 10 μm

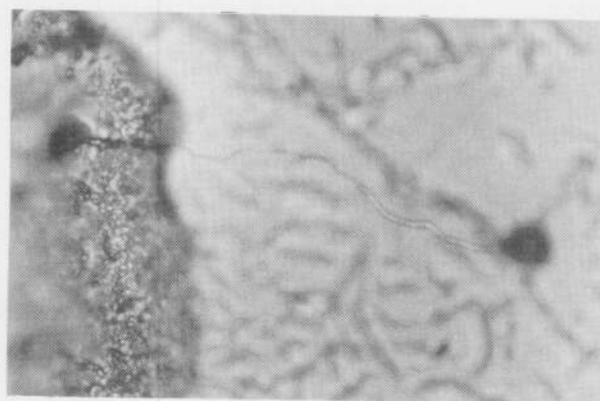


Fig.6 Reflected light : 10 μm

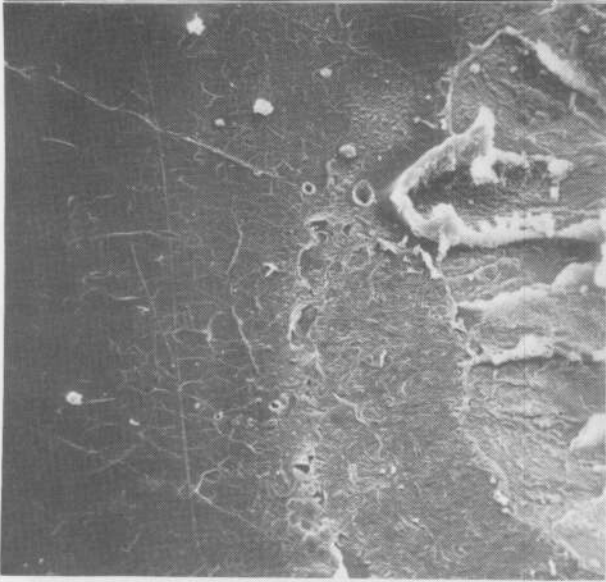


Fig.7 SEM image : 50 μm 

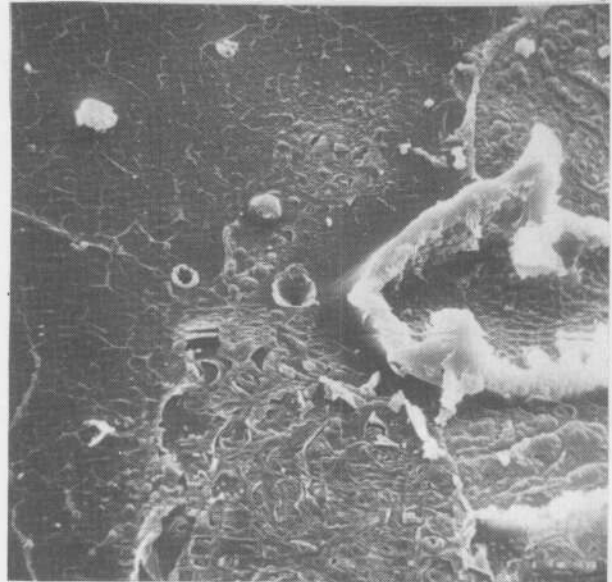



Fig.8 SEM image : 10 μm 

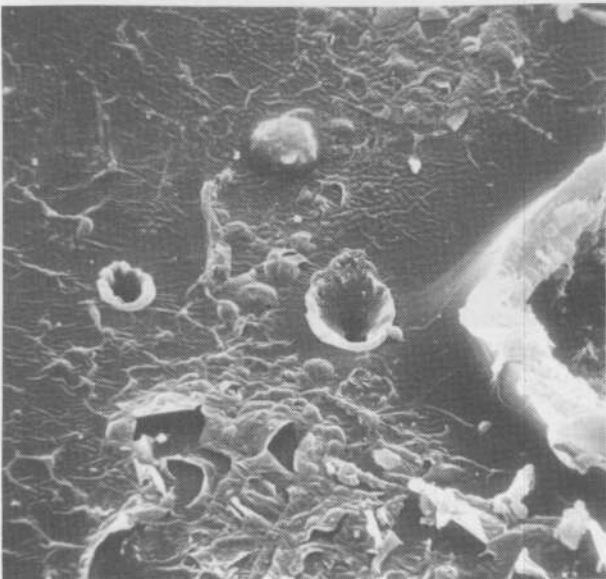


Fig.9 SEM image : 10 μm 

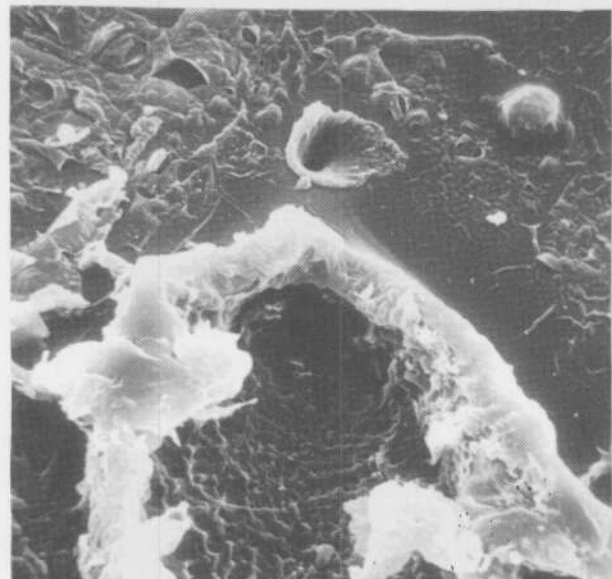


Fig.10 SEM image : 10 μm 

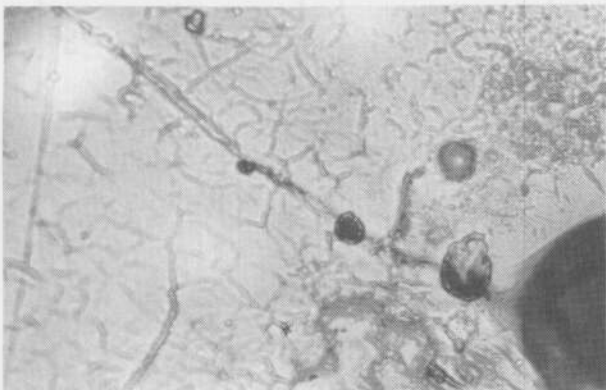



Fig.11 Reflected light : 10 μm 

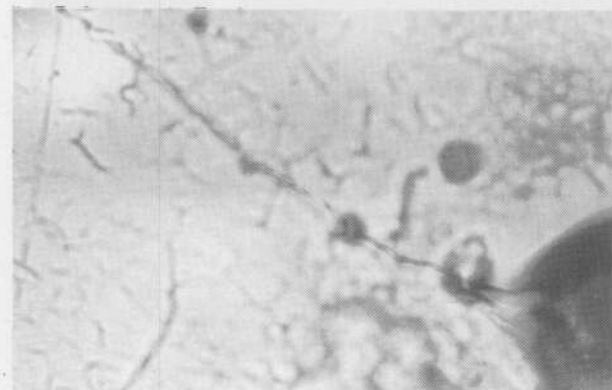



Fig.12 Reflected light : 10 μm 

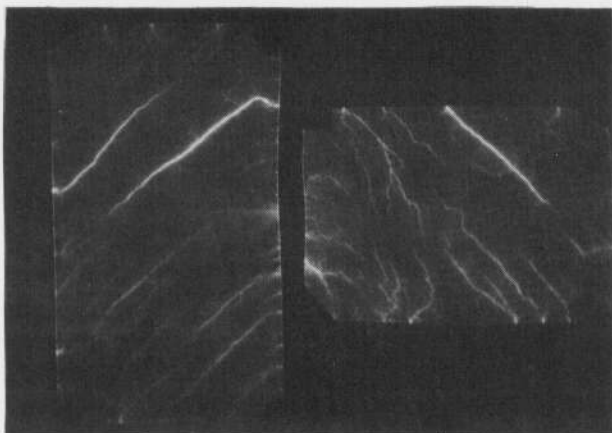


Fig.13 Arc on Mylar

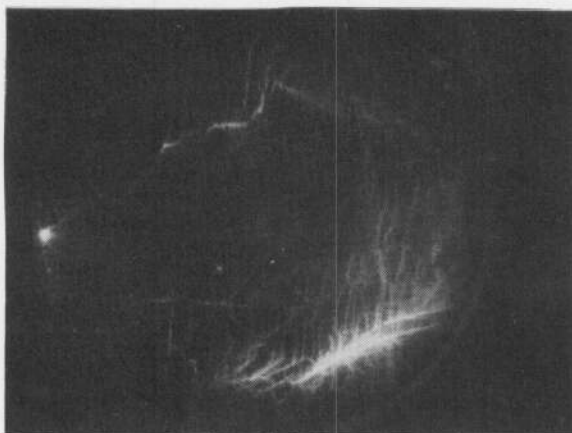


Fig.14 Arc on Teflon

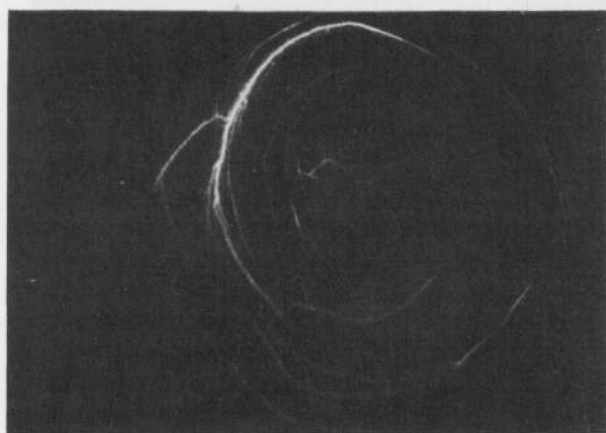


Fig.15 Arc on Teflon

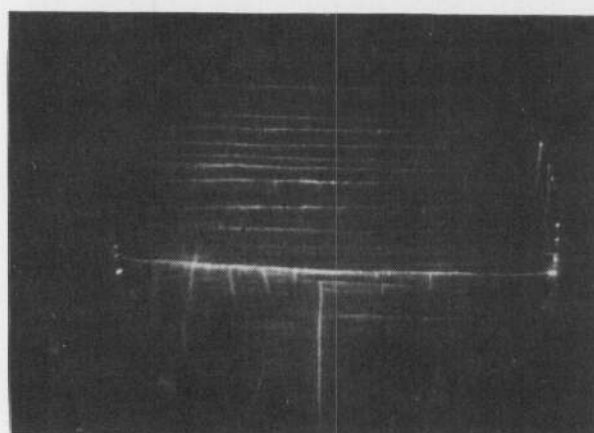


Fig.16 Arc on Teflon

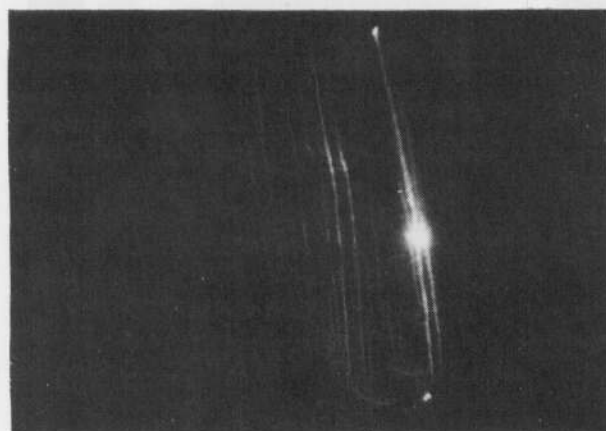


Fig.17 Arc on Teflon

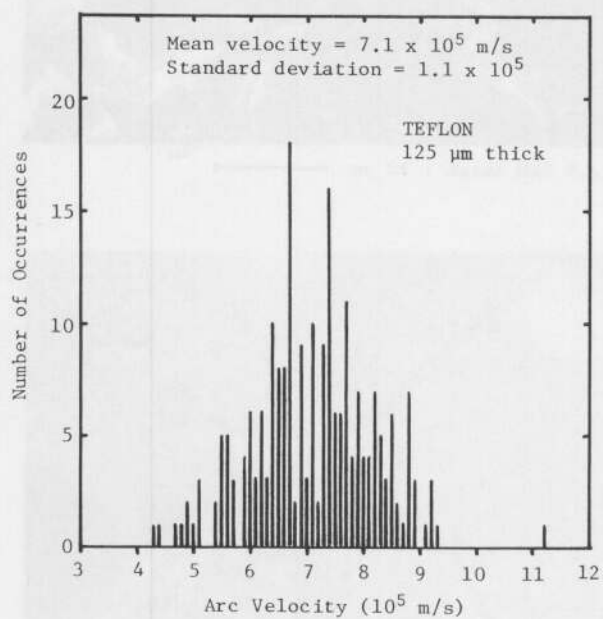


Fig.18 Arc velocity distribution